

## MECHANICAL AND MORPHOLOGICAL PROPERTIES OF STEARATE MODIFIED LAYERED DOUBLE HYDROXIDE BLEND WITH POLYHYDROXYBUTYRATE/POLY(LACTIC ACID) NANOCOMPOSITES

S. N. TEH, M. B. AHMAD\*, K. SHAMELI, N. A. IBRAHIM, N. ZAINUDDIN, Y. Y. THEN

*Department of Chemistry, Faculty of Science, Universiti Putra Malaysia, 43400 UPM Serdang, Selangor, Malaysia*

In this study, poly(3-hydroxybutyrate) (PHB)/poly(lactic acid) (PLA)/stearate modified magnesium aluminum layered double hydroxides (SMALDH) nanocomposites were prepared from PHB/PLA blend and SMALDH by solvent-casting method. The ratio of PHB/PLA was fixed at 90/10 as it gave the optimum tensile properties among the blends. Mg/Al layered double hydroxide (MALDH) was first synthesized via a co-precipitation method from nitrates salt solution and then modified with sodium stearate via an anion exchange process. X-ray diffraction (XRD) result showed an incensement in d-spacing of MALDH from 7.88 to 30.26 Å after it was modified with sodium stearate, suggested that the intercalation of stearate ions into the interlayer of MALDH. The addition of 1.5 wt% of SMALDH improved the tensile strength and tensile modulus of PHB/PLA blend by 23% and 13%, respectively. Those improvements were attributed to the improved interfacial adhesion of blend components as illustrated in scanning electron micrograph. XRD result and transmission electron micrograph showed that the nanocomposites produced are of mixture intercalated/exfoliated types.

(Received April 8, 2014; Accepted June 11, 2014)

*Keywords:* Poly(3-hydroxybutyrate), Poly(lactic acid), Layered double hydroxides, Nanocomposites.

### 1. Introduction

In last two decades, most of the research had focused on the utilization of biodegradable polymers as green materials. Biodegradable polymers are attractive as they can becleave by microorganisms such as bacteria into carbon dioxide and water through chemical or biological reactions [1-4]. Therefore, much scientific research had paid attention on the development and commercialization of biodegradable polymers since it makes significant reduction in environmental impact. However, there is lot of potential in the improvement of biodegradable polymer properties for large scale or mass level applications [5].

Poly(3-hydroxybutyrate) (PHB) is a biodegradable, thermoplastic polyester. It can be produced from renewable resources via bacteria and algae fermentation. It has a high degree of crystallinity and possesses characteristics comparable to that of isotactic polypropylene (PP). It is water insoluble and relatively resistant to hydrolytic degradation compared to those of other biodegradable polyesters. However, its brittleness, low melt viscosity, and thermal instability limit the uses of PHB [6]. Poly(lactic acid) (PLA) is a biodegradable polymer derived from renewable resources such as corn starch or sugarcane. It has various good mechanical properties like high tensile strength, modulus, thermo-plasticity, transparency, and fabric ability [7].

Zhang et. al. [8] had reported the preparation of PHB/PDLLA blends through solution casting method. They found out that there were certain improvements in mechanical properties of PHB after the incorporation of PLA into PHB. However, the authors found out that PHB/PLA

---

\*Corresponding authors: mansorahmad@gmail

blend prepared were immiscible over the range of compositions studied. Consequently, this research was conducted to improve the compatibility of the blend components by applying nanofiller.

Inorganic–organic nanocomposite materials with functional organic compounds immobilized into a layered inorganic matrix have potential to offer scientific and technological advantages, since the organized two-dimensional arrays of organic species between the interlayers can result in novel functions that are different to the typical functions of the individual organic species [9-15].

Layered double hydroxide (LDH) has attracted much attention due to its high anion-exchange capacities [16-19]. The layered structure of LDH make it as an attractive choice as nanofiller for preparation of polymer/layered clay nanocomposites. Magnesium and aluminium were chosen as the LDH metals in this study as they yield more environmental friendly materials [20]. The high charge density and the high contents of interlayer anions and water molecules of LDHs result in strong hydrophilic properties and thus prevent swelling and exfoliation of the LDHs sheets. Therefore, it is hard to be intercalated by the hydrophobic polymer chains and to reach a good level of filler dispersion [21, 23]. For that reason, LDH is often been modified with organic anions to alter the surface LDH hydrophobicity and enlarge the interlayer distance between LDH layer so that the intercalation of polymer chains becomes feasible [7, 20]. Organic anionic surfactants containing at least one anionic end group and a long hydrophobic tail are the most suitable materials for this purpose. Several authors [7] had reported the preparation of nanocomposites using LDH. The nanocomposites showed enhancement in mechanical properties [24, 25] which indicated that the LDH nano-platelets with the polymer matrix exhibited excellent compatibility [10], and improvement in thermal stability [26-28] after blending with LDH.

In this study, the effect of SMALDH addition on the tensile properties of PHB/PLA blend was investigated. The SMALDH was used to improve the compatibility of PHB/PLA blend and at the same time produced nanocomposites with enhanced tensile properties.

## **2. Experimental Section**

### **2.1 Materials**

Bacterial synthesized Poly[(R)-3-hydroxybutyric acid] PHB, was purchased from Sigma-Aldrich, Germany. The Poly(lactic acid) PLA (4060D), was purchased from Nature Works LLC, U.S.A. Magnesium nitrate-6-hydrate ( $\text{Mg}(\text{NO}_3)_2 \cdot 6\text{H}_2\text{O}$ ) was supplied from R&M Chemicals, UK and aluminum nitrate-9-hydrate ( $\text{Al}(\text{NO}_3)_3 \cdot 9\text{H}_2\text{O}$ ) was supplied by HmbG Chemicals, Germany. Sodium hydroxide pellets, (NaOH) which used as a precipitation agent was supplied by Merck, Germany. Counter ionic surfactant, sodium stearate was purchased from R&M chemicals, UK. All the above chemicals were analytical grades and used as received.

### **2.2. Preparation of Stearated Modified Mg/Al LDH (SMALDH)**

Mg/Al LDH (MALDH) was prepared by co-precipitation of mixed metal salts as described by Eili et al. [7]. The metal salts of  $\text{Mg}(\text{NO}_3)_2 \cdot 6\text{H}_2\text{O}$  (0.2M) and  $\text{Al}(\text{NO}_3)_3 \cdot 9\text{H}_2\text{O}$  (0.067M) was first dissolved in 250 mL decarbonated water, giving Mg/Al molar ratio of 3-1 respectively. Later, 1.0M NaOH was added drop wise to the salts solution with vigorous stirring under nitrogen atmosphere to pH 9.0. The precipitate was then aged at 70°C for 16 hours in a water bath shaker. The precipitate was filtered and washed with deionized water for twice. After that, the precipitate was dried in an oven at 60°C. The dried sample was then ground using a mortar and used in modification by sodium stearate. The SMALDH was prepared by replacing nitrate ions in the MALDH layers with stearate ions using the procedure described by Eili et al. [7]. In brief, 1.0g of MALDH was mixed with 0.9194g (0.003 M) sodium stearate in 1000mL deionized water and stirred for 1 hour. After that, the white SMALDH was filtered and washed with 1000mL deionized water for 3 times and dried in oven at 60°C. The dried sample was ground using a mortar and sieved into particle size of less than 100  $\mu\text{m}$ .

### 2.3. Preparation of PHB/PLA/SMALDH Nanocomposites

PHB/PLA/SMALDH nanocomposites were prepared by solvent-casting method using chloroform as solvent. The ratio of PHB/PLA was fixed at 90/10 as this blend exhibited optimum tensile properties among the blends. The preparation procedure was as follow: PHB and PLA was respectively dissolved in 50mL chloroform, and mixed after 1 hour stirring. At the same time, SMALDH was suspended in 50mL chloroform and stirred for 1 hour. The suspension were then mixed with ratio (PHB/PLA/SMALDH) 90/10/0, 90/10/0.5, 90/10/1.0, 90/10/1.5, 90/10/2.0, 90/10/3.0 and 90/10/4.0 wt% and stirred for another one and half hour. After that, the PHB/PLA/SMALDH suspension was poured into Petri dish and dried in the fume cupboard for 4-5 days.

### 2.4. Characterizations

XRD patterns of the LDHs and nanocomposites were recorded using a Shimadzu XRD 600 Diffractometer operated at 30 kV and 30 mA with Cu-K $\alpha$  radiation at wavelength of 1.5405 nm. Data was collected within the range of scattering angles of  $2\theta$  of 2 to 30° at the scan rate of 2°/min. The functional group of LDH, blend and nanocomposites were analyzed by a Spectrum BX Perkin Elmer. Using ATR disc method. The spectra were recorded in the range of frequency of 280 to 4000 cm<sup>-1</sup> at 25°C. Instron Tensile Testing Machine model 4302 was used to test the tensile properties of the blend and nanocomposites. The samples were cut into dumb-bell shape according to ASTM D638-V. Tensile fracture surfaces of the blend and nanocomposites were studied using JEOL scanning microscope JSM-6400, operated at 15 kV. The dispersion of SMALDH in the blend was studied by a transmission electron microscope Hitachi, H7100 with accelerating voltage of 100 kV. The samples were dispersed in chloroform and diluted to the right concentrations. The suspension was then dropped on to the TEM sample grid using a dropper and allowed it to dry. A very thin layer on the grid was then observed under the microscope.

## 3. Results and discussion

MALDH was successfully synthesis by a co-precipitation method from nitrates salt solution. The hydrophilic nature of MALDH makes it incompatible with PHB/PLA blend. Therefore, MALDH was modified with sodium stearate to alter the LDH surface hydrophobicity in order to improve the compatibility and facilitate the intercalation of polymer chains into the SMALDH. The SMALDH produced was then solution casted with PHB/PLA to produce PHB/PLA/SMALDH nanocomposites with improved tensile properties.

### 3.1. Characterizations of SMALDH

#### 3.1.1. X-ray Diffraction (XRD)

The XRD patterns of MALDH and SMALDH in  $2\theta$  range of 2 to 30° are shown in Figure 1. The interlayer spacing,  $d$  of the LDH is calculated from the first diffraction peak (003) using Bragg's equation,  $n\lambda = 2d\sin\theta$ , where  $n$  is equal to 1 for the first diffraction peak (003),  $\lambda$  is the wavelength of Cu-K $\alpha$  radiation, and  $\theta$  is the half of the scattering angle [7, 29].

The interlayer spacing,  $d_{003}$  of MALDH has increased from 7.88 to 30.26Å after modification with sodium stearate. The increase in the basal spacing indicates that the anions are successfully intercalated into the interlayer of LDH as reported by Eili et al. [7], Liu et al. [26], and Pradhan et al. [30].

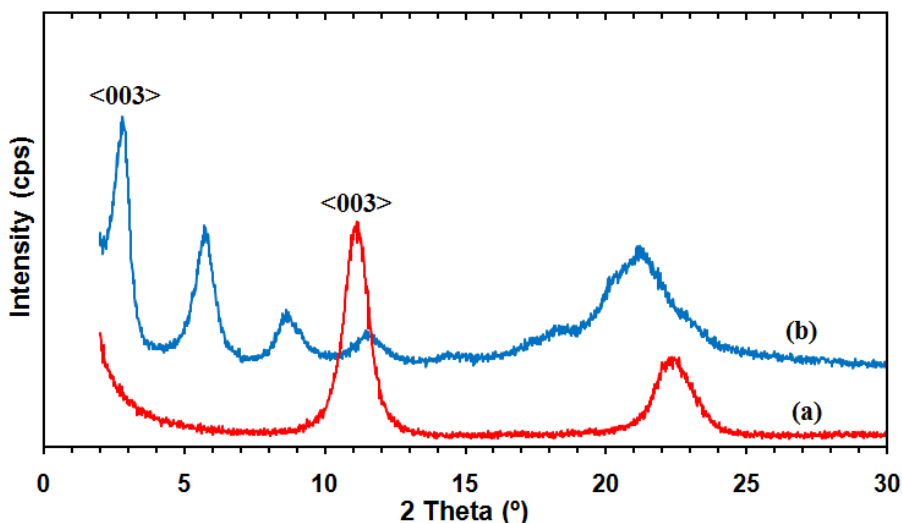


Fig. 1. XRD patterns of (a) MALDH and (b) SMALDH.

### 3.1.2. Fourier Transform Infrared (FTIR) Spectroscopy

Fig. 2 shows the FTIR spectra of MALDH and SMALDH. The common features in both SMALDH and MALDH spectra are peaks observed at  $3511$  and  $3514$   $\text{cm}^{-1}$ , assigned to O-H group stretching of both hydroxide layers and interlayer water molecules. The stretching vibration (H-O-H) of the interlayer water can be observed at about  $1600$ - $1700$   $\text{cm}^{-1}$ . The lattice vibration bands of the M-O and O-M-O (M=Mg or Al) bondings appear at below  $800$   $\text{cm}^{-1}$ . The MALDH also shows an intense band at  $1378$   $\text{cm}^{-1}$ , which can be associated with the asymmetric stretching vibration of the nitrate anion [30-32]. In the SMALDH, it shows some new adsorption bands present at  $2929$  and  $2893$   $\text{cm}^{-1}$  correspond to C-H stretching and  $\text{CH}_2$ ,  $\text{CH}_3$  stretching, respectively [26]. The presence of new adsorption bands are the characteristic absorptions of the C-H stretching vibration of the  $\text{CH}_3$  and  $\text{CH}_2$  groups of long chain stearate anions [33]. It also indicates two strong adsorption peaks of the carboxylate asymmetric and symmetric stretching which locate at  $1561$  and  $1426$   $\text{cm}^{-1}$ , respectively [34, 35].

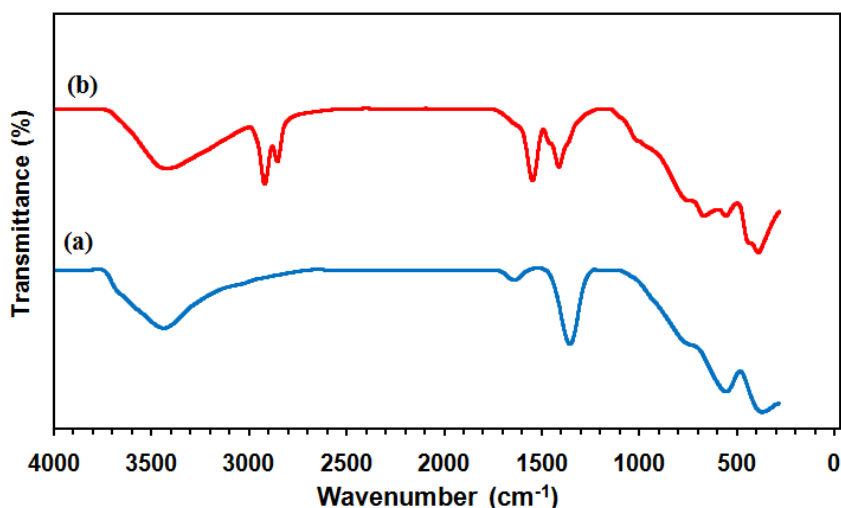


Fig. 2. FTIR spectra for (a) MALDH and (b) SMALDH.

### 3.1.3. Scanning Electron Microscopy (SEM)

Surface morphology of the MALDH and SMALDH particles are shown in Figure 3. Figure 3(a) shows that the LDH nano-sheets severely aggregated and formed very big particles

[25]. After modification with sodium stearate, the SMALDH shows decreased in particle size with smaller agglomerates of compact and non-porous granule structure (Figure 3(b)) [23].

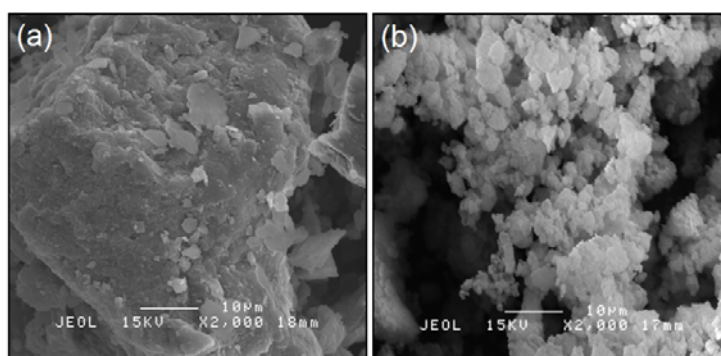


Fig. 3. Scanning electron micrograph of (a) MALDH and (b) SMALDH.

### 3.2. Characterizations of PHB/PLA/SMALDH Nanocomposites

#### 3.2.1. X-Ray Diffraction (XRD)

Fig. 4 shows the XRD patterns of PHB, PLA, PHB/PLA and PHB/PLA/SMALDH nanocomposites. The PHB shows two strong diffraction peaks at  $2\theta$  of  $13.94^\circ$  and  $17.24^\circ$ , which corresponds to the 020 and 110 planes of orthorhombic structure, respectively whereas the PLA shows a typical amorphous broad band [36]. Generally, the XRD pattern of PHB/PLA blend is very similar to that of PHB (Figure 4 (c)) [36, 37]. The shift and broaden in peak of the blend may due to the addition of PLA to PHB change the crystal phase of the PHB samples. This indicates that the presence of amorphous PLA reduces the crystallinity of the PHB [38]. The XRD patterns of all PHB/PLA/SMALDH nanocomposites are very similar to that of PHB/PLA blend. The characteristic peak of the SMALDH in the nanocomposites is absent, mainly attributed to that of the loading of the SMALDH in the nanocomposites is too low or exfoliated into single layer [39].

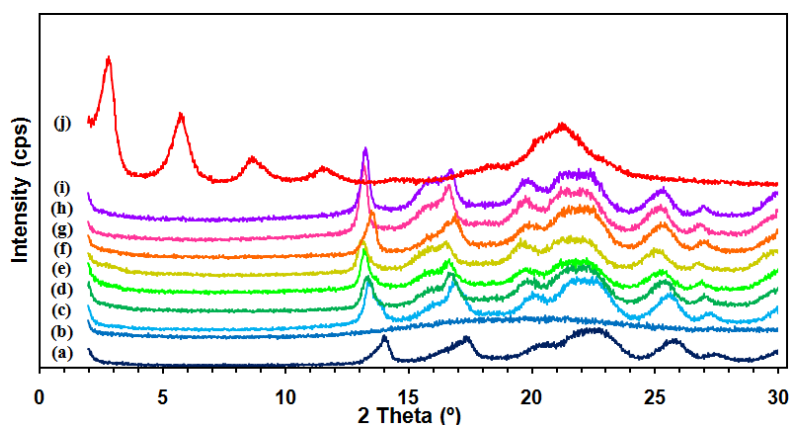


Fig. 4. XRD patterns of (a) PHB, (b) PLA (c) PHB/PLA and the nanocomposites with (d) 0.5, (e) 1.0, (f) 1.5, (g) 2.0, (h) 3.0 and (i) 4.0 wt% SMALDH content and (j) SMALDH.

#### 3.2.2. Fourier Transform Infrared (FTIR) Spectroscopy

Figure 5 shows the FTIR spectra of PHB, PLA, PHB/PLA blend and nanocomposites at various ratios. Both PHB and PLA spectrum showed common peak of the  $\text{CH}_3$  asymmetric deformation at  $1452\text{ cm}^{-1}$  and  $\text{CH}_3$  symmetric deformation at  $1377\text{ cm}^{-1}$  and  $1361\text{ cm}^{-1}$ , respectively. In the spectrum of PHB, there is a strong absorption peak at  $1720\text{ cm}^{-1}$  which is related to the stretching vibrations of crystalline carbonyl groups,  $\text{C}=\text{O}$  stretching. However the amorphous carbonyl vibration of PHB at  $1740\text{ cm}^{-1}$  is too weak and cannot clearly observed in the

spectrum [37, 40]. There is a strong peak at  $1748\text{ cm}^{-1}$  which can clearly be observed in the spectrum of PLA indicates that the stretching vibrations of crystalline carbonyl groups. Conversely the crystalline carbonyl vibration of PLA at  $1755\text{ cm}^{-1}$  is very weak and is hard to detect by the FTIR spectrometer [40]. It is clear that the band width of PHB and PLA for C=O carbonyl stretching is vary from each other due to the state order of both polymer is different as PHB is highly crystalline and PLA is primarily amorphous [41]. The spectrum of PHB/PLA blend is similar to that of PHB and PLA spectra. This is due to the similarity in chemical structure and functional group of PHB and PLA [40]. There is not much different between the spectra of the nanocomposites and PHB/PLA blend. The characteristic peak of the SMALDH in the nanocomposites is hard to be detected due to low filler loading. There is no major peak shifting or formation of new peak in the nanocomposites indicating there are no strong interactions between them [37, 42].

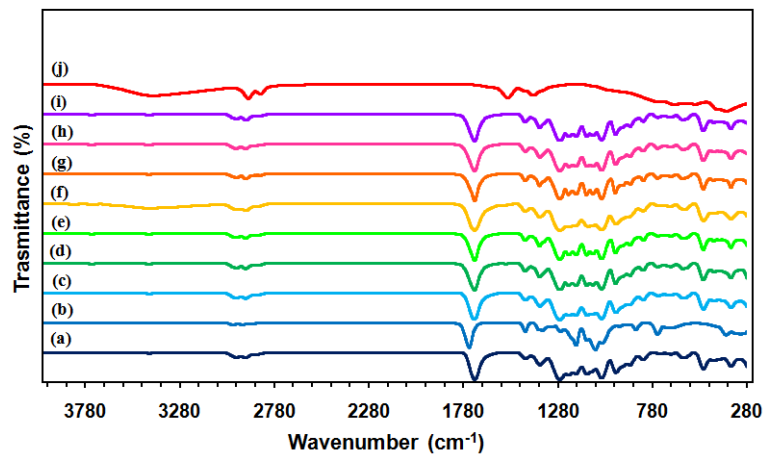


Fig. 5. FTIR spectra of (a) PHB, (b) PLA (c) PHB/PLA and the nanocomposites with (d) 0.5, (e) 1.0, (f) 1.5, (g) 2.0, (h) 3.0 and (i) 4.0 wt% SMALDH content and (j) SMALDH.

### 3.2.3. Tensile Properties

Tensile strength of PHB/PLA/SMALDH nanocomposites as a function of SMALDH content is illustrated in Figure 6 and Figure 7. Pristine PHB shows a tensile strength of 23.20 MPa, tensile modulus of 562.55 MPa and elongation at break of 20.80%. It shows that PHB is a brittle material which exhibit slow melt viscosity and high modulus. Blending of PLA into PHB improved the tensile properties of PHB. Both tensile strength and tensile modulus increase to an optimum value of 28.27 MPa and 651.83 MPa, respectively when the 10 wt% PLA is blended with PHB. It also shows improvement in elongation at break as compared to that of PHB. This indicates that PLA is able to improve the mechanical properties of PHB. Thus this ratio is chosen for further investigation in the nanocomposites. The improvement in mechanical properties in the PHB/PLA blends may be due to the possible interaction between PHB and PLA causing strong interfacial bonding [38].

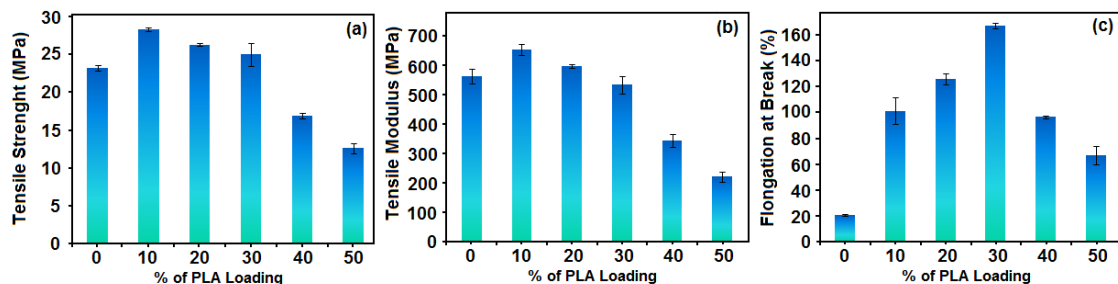


Fig. 6. The tensile strength (a), tensile modulus (b) and elongation at break (c) of PHB/PLA blends as a function of PLA content.

The tensile strength of the nanocomposites increases with increasing SMALDH content until it reaches optimum value at 1.5 wt% of SMALDH. After that, the tensile strength decreases gradually as the loading of the SMALDH increases. The presence of 1.5 wt% SMALDH improves the tensile strength of the PHB/PLA blend by 22%. The interactions between SMALDH and polymer matrix strongly affected the tensile strength of the nanocomposites. The compatibilization at molecular level depended on the interfacial adhesion at the phase boundaries [43]. The increased in the tensile strength of the nanocomposites shows that the interfacial adhesion of SMALDH and PHB/PLA blend increased. This indicated that the compatibility of PHB/PLA blend had been improved by adding SMALDH. Same trend is also observed in the tensile modulus of the nanocomposites. The tensile modulus increases to optimum value when 0.5 wt% SMALDH was added into the blend, then decreases gradually as the SMALDH content increases. The tensile modulus is improved by 26% with the presence of 0.5 wt% SMALDH. After it reaches optimum value, the reductions in tensile strength and tensile modulus are attributed to the aggregation of the SMALDH [7] which induces a local stress concentration inside the blend [44].

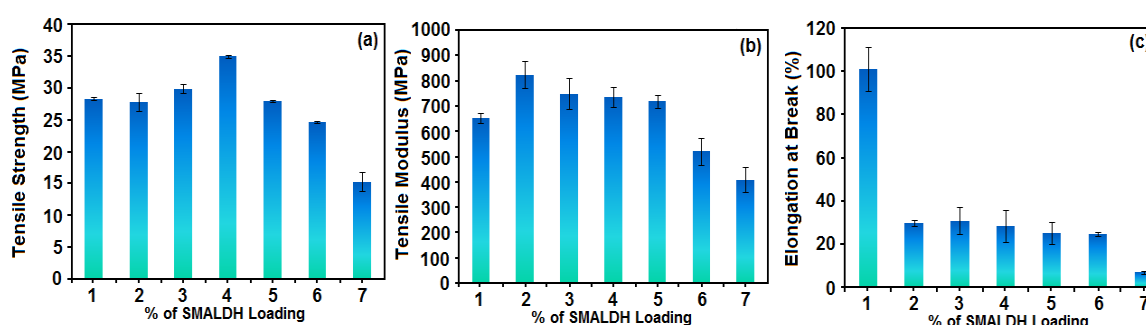


Fig. 7. The tensile strength (a), tensile modulus (b) and elongation at break (c) of PHB/PLA/SMALDH nanocomposites as a function of SMALDH content.

Blending of SMALDH into the polymer blend also decreases the elongation at break of the blend. The decrease in elongation at break is attributed to the presence of SMALDH in the PHB/PLA blends that restricts the mobility of the polymer chain or deformability of a rigid interface between SMALDH and polymer matrix [45-48]. There has been a general agreement that polymer-based clay nanocomposites are much more brittle than their neat polymer counterparts [42].

#### 3.2.4. Scanning Electron Microscopy (SEM)

The morphologies of the tensile fracture surfaces of the PHB, PLA, PHB/PLA blend and nanocomposites at various loading of SMALDH at magnification of 2000X are shown in Figure 7. Pure PHB (Figure 8a) shows an irregular fracture surface due to its crystallinity [36, 37], whereas the pure PLA (Figure 8b) shows a smooth and uniform surface of an amorphous polymer which indicated that PLA is flexible. The PHB/PLA blends show different fracture surface compared to PHB as the amorphous PLA is blended with it (Figure 8c). The irregular fracture surface of the PHB is hard to see in the SEM micrograph of the blends. These shows after blending PLA to PHB, the fracture surface of PHB had been modified. The blends are expected to have better fracture toughness compared to PHB [38].

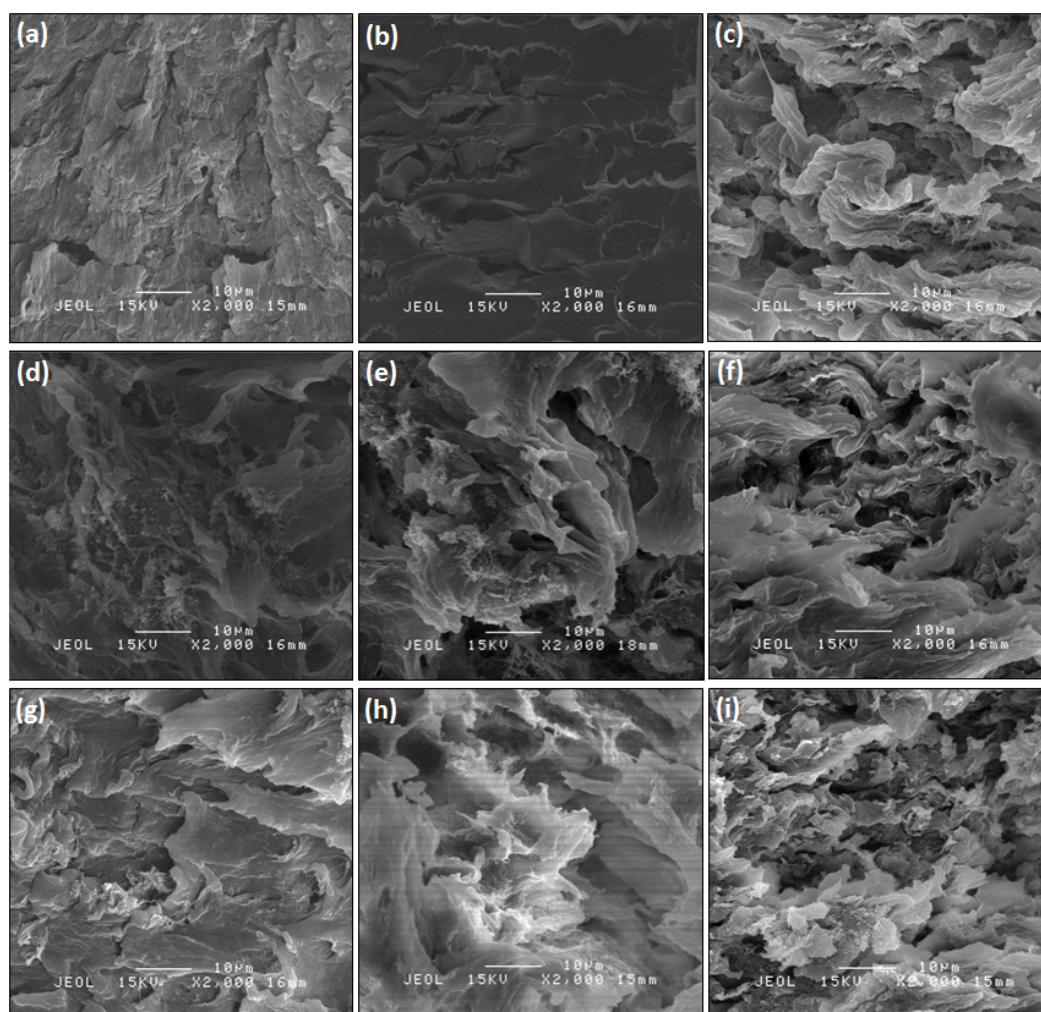


Fig. 8. The fracture morphology of (a) PHB, (b) PLA, (c) PHB/PLA, and the nanocomposites with (d) 0.5, (e) 1.0, (f) 1.5, (g) 2.0, (h) 3.0 and (i) 4.0 wt% SMALDH content.

The morphology of the tensile fracture surface of the PHB/PLA blend change after addition of SMALDH (Figure 8d-i). It is obvious that there are no agglomeration of SMALDH can be observed. In addition, compared to the plain PHB/PLA blend, the fracture surface became smooth with the presence of SMALDH. This suggested the brittle fracture of the nanocomposites which supported the reason of gradually decrease in elongation at break with the presence of SMALDH in the nanocomposites. The brittle behavior of the nanocomposites is probably originated from the formation of micro-voids due to the de-bonding of LDH nanoplatelets from the polymer matrix upon failure [24].

### 3.2.5. Transmission Electron Microscopy (TEM)

Figure 9 illustrates the TEM image of the formation of nanocomposite with 1.5 wt% of the SMALDH. The dark lines represent the SMALDH layers in the PHB/PLA blends matrix. The TEM image shows stacking of SMALDH which indicates the present of intercalated structure. In addition to small stacks of intercalated SMALDH, exfoliated sheets of SMALDH which are not well ordered and randomly distributed in the PHB/PLA matrix are also observed, consistently with formation of an intercalated/exfoliated structure [23, 31, 35].

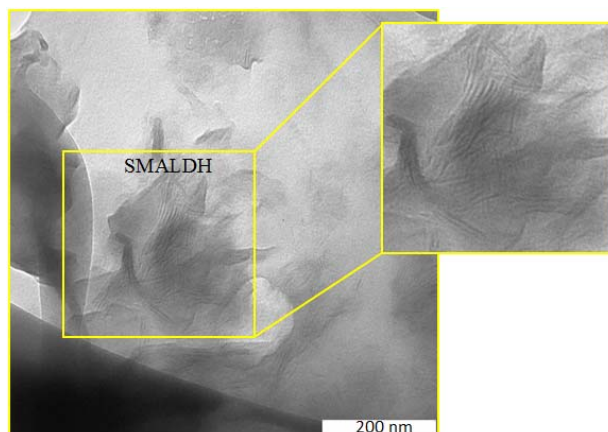


Fig. 9. TEM image of PHB/PLA-SMALDH nanocomposites with 1.5 wt% SMALDH content.

#### 4. Conclusions

MALDH was successfully prepared by a co-precipitation method via an ion-exchange method, using sodium stearate as modifier. The FTIR and XRD results showed that the stearate anion has successfully intercalated into MALDH. The PHB/PLA blend and PHB/PLA/SMALDH nanocomposites were successfully prepared by solvent casting method. TEM micrograph showed that the nanocomposites produced are of intercalated/exfoliated type. The presence of 1.5 wt% of SMALDH showed highest tensile strength among the other ratios by improvement about 22% compared to the plain PHB/PLA blends.

#### Acknowledgements

The authors would like to acknowledge the financial support from Universiti Putra Malaysia (UPM) (RUGS Project No. 9199840). They are also grateful to the staff of the Department of Chemistry UPM and the Institute of Bioscience UPM for the technical assistance.

#### References

- [1] M.S. Usman, N.A. Ibrahim, K. Shameli, N. Zainuddin, W.M.Z. Wan Yunus. *Molecules* **17**, 14928 (2012).
- [2] M.B. Ahmad, Y. Gharayebi, M.S. Salit, M.Z. Hussein, K. Shameli. *Int. J. Mol. Sci.* **12**(9), 6040 (2011).
- [3] M.B. Ahmad, J.J. Lim, K. Shameli, N.A. Ibrahim, M.Y. Tay. *Molecules* **16**(9), 7237 (2011).
- [4] K. Shameli, M.B. Ahmad, P. Shabanzadeh, E.A.J. Al-Mulla, A. Zamanian, Y. Abdollahi, S.D. Jazayeri, M. Eili, F.A. Jalilian, R.Z. Haroun. *Res. Chem. Intermed.* **40**, 1313 (2013).
- [5] U.H. Park, M. Ye, K. Park. *Molecules* **10**, 146 (2005).
- [6] H. Verhoogt, B.A. Ramsay, B.D. Favis. *Polymer* **35**, 5155 (1994).
- [7] M. Eili, W.M.Z. Wan Yunus, Z. Hussien, M. Ahmad, N.A. Ibrahim. *J. Appl. Polym. Sci.* **118**, 1077 (2010).
- [8] L.; Zhang, C.; Xiong, X. Deng. *Polymer* **37**, 235 (1996).
- [9] R. Khandanlou, M.B. Ahmad, K. Shameli, K. Kalantari. *Molecules* **18**(6), 6597 (2013).
- [10] K. Shameli, M.A. Ahmad, E.A.J. Al-Mulla, P. Shabanzadeh, S. Bagheri. *Res. Chem. Intermed.* **1** (2013). (DOI 10.1007/s11164-013-1188-y)
- [11] P. Shabanzadeh, K. Shameli, M. Mohaghehtabar. *Dig. J. Nanomater. Bios.* **8**(3), 1133 (2013).
- [12] Y. Abdollahi, A. Zakaria, A.H. Abdullah, H.R.F. Masoumi, H. Jahangirian, K. Shameli,

- M. Rezayi. *Chem. Cent. J.* **6**(1), 1 (2012).
- [13] K. Kalantari, M.A. Ahmad, K. Shameli, R. Khandanlou, *Int. J. Nanomed.*, **8**, 1817 (2013).
- [14] K. Shameli, M.B. Ahmad, S.D. Jazayeri, P. Shabanzadeh, P. Sangpour, H. Jahangirian, *Chem. Cent. J.* **6**(1), 1 (2012).
- [15] M.B. Ahmad, J.J. Lim, K. Shameli, N.A. Ibrahim, M.Y. Tay, B.W. Chieng, *Chem. Cent. J.* **6**(1), 1 (2012).
- [16] M.; Eili, K.; Shameli, N.A.; Ibrahim, W.M.Z. Wan Yunus, *Int. J. Mol. Sci.* **13**, 7938 (2012).
- [17] Y.L. Pak, M.B. Ahmad, K. Shameli, W.M.Z. Wan Yunus, N.A. Ibrahim, N. Zainuddin. *J. Nanomater.* **1** (2013). (<http://dx.doi.org/10.1155/2013/621097>)
- [18] Y.L. Pak, M.B. Ahmad, K. Shameli, W.M.Z. Wan Yunus, N.A. Ibrahim, N. Zainuddin. *Dig. J. Nanomater. Bios.* **8**(4), 1395 (2013).
- [19] C.P. Liau, M.B. Ahmad, K. Shameli, W.M.Z. Wan Yunus, N.A. Ibrahim, N. Zainuddin, Y.Y. Then. *Sci. World J.* **1** (2014). (<http://dx.doi.org/10.1155/2014/572726>)
- [20] C. Manzi-Nshuti, P. Songtipya, E. Manias, J-G. Maria, M.H. Jeanne, C. Wilkie. *Polymer* **50**, 3564 (2009).
- [21] S.P. Newman, W. Jones. *New J. Chem.* **22**, 105 (1998).
- [22] F. Malherbe, J.P. Besse. *J. Solid State Chem.* **155**, 332 (2000).
- [23] T.Y. Tsai, S.W. Lu, Y.P. Huang, F.S. Li. *J. Phys. Chem. Solids* **67**, 938 (2006).
- [24] H. Peng, W.C. Tjiu, L. Shen, S. Huang, C. He, T. Liu. *Compos. Sci. Technol.* **69**, 991 (2009).
- [25] Q. Wang, X. Zhang, C.J. Wang, J. Zhu, Z. Guo, D. O'Hare. *J. Mater. Chem.* **22**, 19113 (2012).
- [26] J. Liu, G. Chen, J. Yang. *Polymer* **49**, 3923 (2008).
- [27] W. Cui, J.Y. Zhao, H. Li, H. Liu, M. Zhou. *EXPRESS Polym. Lett.* **6**, 485 (2012).
- [28] Chen, W. Feng, L. Qu, B. *Solid State Commun.* **130**, 259 (2004).
- [29] L. Du, B. Qu. Y. Meng, Q. Zhu. *Compos. Sci. Technol.* **66**, 913 (2006).
- [30] S. Pradhan, F.R. Costa, U. Waganknecht, D. Jehnichen, A.K. Bhowmick, G. Heinrich. *Eur. Polym. J.* **44**, 3122 (2008).
- [31] M. Kotal, S.K. Srivastara, A.K. Bhowmick, S.K. Chakraborty. *Polym. Int.* **60**, 772 (2010).
- [32] F.R. Costa, B.K. Satapathy, U. Wagenknecht, R. Weidisch, G. Heinrich. *Eur. Polym. J.* **42**, 2140 (2006).
- [33] C. Nyambo, P. Songtipya, E. Manias, M.M. C.A. Jimenez-Gascoc Wilkie. *J. Mater. Chem.* **18**, 4827 (2008).
- [34] H.B. Hsueh, C.Y. Chen. *Polymer* **44**, 1151 (2003).
- [35] C. Nyambo, P. Songtipya, E. Manias, M.M. Jimenez-Gasoo, C.A. Wilkie. *J. Mater. Chem.* **18**, 4827 (2008).
- [36] A.M. Abdelwahab, A. Flynn, B.S. Chiou, S. Imam, W. Orts, E. Chielline. *Polym. Degrad. Stabil.* **97**, 1822 (2012).
- [37] M. Zhang, L.T. Noreen, *Adv. Polym. Tech.* **30**(2), 67 (2011).
- [38] B. Lepoittevin, M. Devalckenaere, N. Pantoustier, M. Alexandre, D. Kubies, C. Calberg, R. Jérôme, P. Dubois. *Polymer* **43**, 4017 (2002).
- [39] B.W. Chieng, N.A. Ibrahim, W.M.Z. Wan Yunus. *EXPRESS Polym. Lett.* **4**, 404 (2010).
- [40] T. Furukawa, H. Sato, R. Murakami, J. Zhang, Y.X. Duan, I. Noda, S. Ochiai, Y. Ozaki. *Macromolecules* **38**, 6445 (2005).
- [41] C. Vogel, E. Wessel, H.W. Siesler. *Biomacromolecules* **9**, 523 (2008).
- [42] Y.Y. Then, N.A. Ibrahim, W.M.Z. Wan Yunus. *J. Polym. Environ.* **19**, 535 (2011).
- [43] H. Essawy, El-Nashar, D. *Polym. Test* **23**, 803 (2004).
- [44] J. K. Mishra, G.H. Kim, I. Kim, I.J. Chung, C.S. Ha. *J. Polym. Sci. Pol. Phys.* **42**, 2900 (2004).
- [45] S. Mahmoudian, M.Z. Wahit, A.F. Ismail, A.A. Yusuf. *Carbohydr. Poly.* **88**, 1251(2012).
- [46] X.V. Cao, H. Ismail, A.A. Rashid, T. Takechi, T. Vo-Huu. *BioResources.* **6**(3), 3260 (2011).
- [47] L. Du, B. Qu. *J. Mater. Chem.* **16**, 1549 (2006).
- [48] N. Tudorachi, C.N. Cascaval, M. Rusu, M. Pruteana. *Polym. Test.* **19**, 785 (2000).